Eur. Phys. J. A (2012) **48**: 12
DOI 10.1140/epja/i2012-12012-y

THE EUROPEAN PHYSICAL JOURNAL A

Regular Article – Experimental Physics

Precise energy of the 9.4 keV gamma transition observed in the ^{83}Rb decay

M. Slezák[1,a], D. Vénos[2], O. Lebeda[2], and T. Trojek[3]

[1] Faculty of Mathematics and Physics, Charles University, CZ-121 16 Prague, Czech Republic
[2] Nuclear Physics Institute, Academy of Sciences of the Czech Republic, CZ-250 68 Řež near Prague, Czech Republic
[3] Faculty of Nuclear Sciences and Physical Engineering, Czech Technical University in Prague, CZ-115 19, Czech Republic

Received: 23 September 2011 / Revised: 12 January 2012
Published online: 8 February 2012 – © Società Italiana di Fisica / Springer-Verlag 2012
Communicated by A.A. Korsheninnikov

Abstract. The energy of the 9.4 keV γ-transition observed in the ^{83}Rb decay was established to be 9405.8(3) eV. This energy value was obtained from photon spectrometry measurements of the differences in the energies of closely spaced lines. The result allows one to determine more precisely the energy of conversion electrons of the 9.4 keV transition, which represent a unique tool for energy calibration of the tritium beta spectrum and systematic measurements in the KATRIN neutrino mass determination experiment.

1 Introduction

The question of the neutrino rest mass is one of the most important problems in modern particle physics, astrophysics and cosmology. The accepted value of $2\,\mathrm{eV}/c^2$ [1] for the upper limit of the rest mass of the electron antineutrino is based on experimental results of $2.3\,\mathrm{eV}/c^2$ [2] and $2.1\,\mathrm{eV}/c^2$ [3] obtained from the analysis of the continuous β-spectrum of tritium in the region near its endpoint.

The aim of the new project KATRIN (KArlsruhe TRItium Neutrino experiment) [4], which is based on the accumulated experience of the earlier experiments, is to improve the sensitivity to the rest mass of the electron antineutrino to $0.2\,\mathrm{eV}/c^2$ (with 90% confidence level) after 1000 days of data taking. The KATRIN electron spectrometer will measure only narrow region of tritium beta spectrum, namely $(E_0 - 30, E_0 + 5)\,\mathrm{eV}$, where $E_0 = 18575.0\,\mathrm{eV}$ denotes the energy of the spectrum endpoint. Test and systematic measurements with monoenergetic electron sources are planned in order to understand the properties of the KATRIN electron spectrometer.

The conversion electrons of 9.4 and 32.2 keV transitions observed in the decay of the isomeric state $^{83\mathrm{m}}$Kr (the daughter nucleus of ^{83}Rb) proved to be useful in previous tritium neutrino experiments [5–10]. Currently, the conversion electrons from subshell K of the 32 keV transition, *i.e.* K-32 electrons, with energy of 17.8 keV relatively close to the E_0 will be used for the monitoring and calibration of the KATRIN energy scale as an alternative method to the standard approach using high-voltage divider with voltmeter [4]. The energies of other conversion electrons encountered in the decay are more remote from E_0, *e.g.*, L_3-32 and L_1-9.4 conversion electrons have energies of 30.5 and 7.5 keV, respectively. These electron lines can be used for refinement of the energy calibration in the tritium beta spectrum endpoint region. Thus the value of E_0, also determined from tritium experiment, can be obtained with smaller uncertainty. The comparison of E_0 with ^{3}H$-^3$He mass difference determined by Penning trap measurement represents a very important cross-check of the tritium neutrino experiments [4]. Besides, overall check of the spectrometer at a broader energy interval will be possible. For this purpose, a high precision of the energies of the conversion electrons is desirable. Moreover, the very narrow electron conversion line N_1-9.4 (the width of only 0.19 eV [8]) with energy of 9.4 keV and relatively high intensity of 1.4% can be used for check of the KATRIN spectrometer response function[1].

The calibration and tests indicated above will be possible without restrictions before the first injection of tritium into the KATRIN windowless tritium source. After that the huge tritium continuous beta spectrum (reduced only by two orders of magnitude when the tritium injection is closed [13]) practically precludes the 9.4 conversion electrons experiments. Eventual measurement with very strong ^{83}Rb/$^{83\mathrm{m}}$Kr source has to be tested. On the other hand, the planned test measurement with condensed krypton source will be possible without limitation. In this

[a] e-mail: slezak@ujf.cas.cz

[1] The intensity is calculated using 9.4 γ-transition intensity from [11] and related conversion coefficient according to [12].

case, the tritium source can be uncoupled by a valve. The 9.4 conversion electrons will be further measured (less frequently) at the monitoring spectrometer additionally to K-32 electron spectra (used specifically for the monitoring of the KATRIN energy scale). In this measurement the high-voltage divider will be common for main and monitoring KATRIN spectrometers. The reason for possible unexpected shift of line positions can be identified: the change of the divider scale factor, if the shift for the higher energy line is larger than that for the lower energy one (scale factor has multiplicative character in calculation of the line position), or change of the work function of the monitoring spectrometer, if the shifts are the same for the lines (the work function has additive character in calculation of the line position).

The energy of a conversion electron emitted from a free krypton atom is given by the difference between the energy of the gamma transition and the relevant subshell atomic electron binding energy plus small corrections ($\leq$ 0.2 eV) that take into account recoil energies. Accuracy of the binding energies for the subshells of free krypton atom is in the subelectronvolt range, see original works [14–21] and reviews [22–25]. The energy of the 9.4 keV transition $E_{9.4}$ has been determined by several authors using gamma spectrometry as 9400(20), 9400(10) and 9390(10) eV in [26,27,11]. Other results, more precise, were obtained using conversion electron spectrometry as 9396(3), 9405.9(8) eV [28,8]. For the condensed ^{83m}Kr electron source [8], an appropriate value was obtained using theoretical corrections for the binding energies. In dissertation [29], the value of 9404.71(35) eV is reported. In this case, the correction of binding energies (1.74 ± 0.23 eV) for the condensed source was taken from photoelectron and Auger electron spectroscopy study [30]. We were motivated to remeasure the value $E_{9.4}$ by photon spectrometry in order to improve its reliability and precision. The method used in this work is similar to that applied in measurement of precise energy of the 32 keV transition [31].

2 Experimental method

The value of $E_{9.4}$ was determined by photon spectrometry measurements of differences in energies of closely spaced photon lines (the method was also described in [32]) using ^{83}Rb/^{83m}Kr source. In the source, the short-lived isomeric state ^{83m}Kr is continuously generated in the decay of ^{83}Rb nuclide. This pure electron capture decay with a half-life of 86.2 d feeds the excited states and stable ground state of ^{83}Kr. In the decay, the 9.4 keV transition, connecting the first excited state and ground state of ^{83}Kr, is fed directly via the electron capture (6%), from the isomeric state ($T_{1/2}$ =1.83 h) (77%) and from the other excited states in ^{83}Kr (17%). Its gamma ray intensity amounts to 5.9%, the rest of the transition intensity is balanced with internal conversion electrons (transition multipolarity is $M1+E2$ with mixing parameter $\delta = 0.0130(8)$). The other decay properties can be found in [33] and [34].

The parent ^{83}Rb was produced at the Řež U-120M cyclotron via the reaction ^{nat}Kr(p,xn)^{83}Rb using a pressurized water cooled krypton gas target. The ^{83}Rb deposited on the target walls was washed out into de-ionized water ($\geq$ 18 MΩ·cm). For the details, see [35]. The solution of rubidium was further cleaned using ion-exchange chromatography. Finally, the ^{83}Rb/^{83m}Kr source for gamma and X-ray measurement was prepared by evaporation of the ^{83}Rb water solution on polyethylene foils. Activity of about 3.5 MBq was placed on a circle with a diameter of $\leq$ 5 mm. The radioactive spot was sealed up by a colorless scotch tape. The retention of gaseous ^{83m}Kr in such a source was in the range of 75–100%, *i.e.* not very far from the amount given by transient equilibrium between the mother and daughter nuclides.

The energy of the 9.4 keV transition in ^{83}Rb was determined by calibration of the detector energy scale with characteristic X-ray lines Kα_1 of nickel and arsenic with energies of 7478.2521(45) and 10543.2674(81) eV [24]. The "calibration" spectra were obtained by fluorescence induced predominantly by the KX-rays of ^{83}Kr when Ni 0.025 mm foil (purity 99.999%) and As powder (purity 99.999%, the As powder was sealed in the scotch tape capsule) were added to the ^{83}Rb/^{83m}Kr source. The distance between the source with fluorescent elements and detector crystal was 80 mm. In order to reduce spectral photon line asymmetry due to incomplete detector charge collection (at the detector edge), an aluminum collimator, with diameter of 6 mm and height of 50 mm, was inserted between the source and the detector.

The photons were detected by commercial apparatus. A 80 mm^2 × 5 mm Si(Li) detector with built-in preamplifier and amplifier was used —both devices were purchased from the Canberra (models SL80175 and 2026, respectively). The computer based ADC card TRUMP from EG&G Ortec digitized the amplifier output signals into 8192 channels. The gain of the amplifier was set to 6.5 eV per channel. The energy resolution of the system, full width at half maximum, was 225 eV at the energy of 9.4 keV.

More than a hundred spectra in different arrangements with different sources ^{83}Rb/^{83m}Kr, ^{81}Rb and ^{241}Am were measured until the satisfactory experimental conditions for the measurement of the actual calibration spectra were found. The crucial findings of this preparation stage were: 1) suitable detector load in order to achieve linear background in the spectral regions of interest, 2) the separate spectra for the determination of the line asymmetry parameters for every region of interest (see text below), 3) relatively large spectroscopy gain (6.5 eV/channel) in order to achieve reproducible results of the line fits for different spectra, 4) partial understanding of the 9.7 keV parasitic line (see the text below). The spectrum measurement time in the preparation stage described above and also for the final calibration spectra was of 10–24 h.

The method using the calibration and calibrated lines very close to each other in energy and measured in one spectrum, if possible, is very effective for the line energy determination with high precision in semiconductor

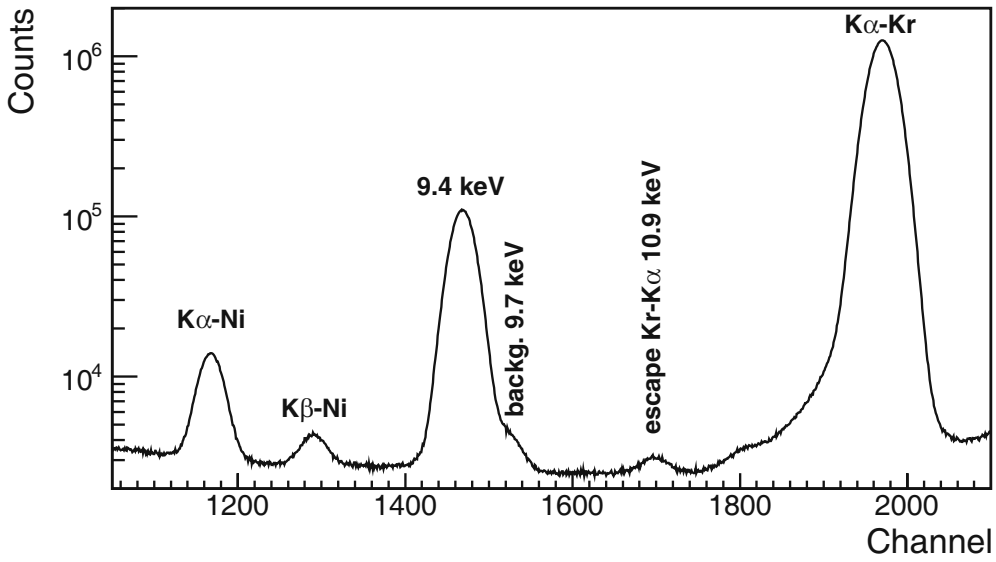

Fig. 1. Partial photon spectrum of the ^{83}Rb/^{83m}Kr source measured with the Si(Li) detector. Besides the expected lines, also the KX lines of Ni and the background line with energy 9.7 keV are visible.

gamma-ray spectrometry. The possible drifts of the line positions and nonlinearity of the spectrometer is heavily reduced in comparison with other methods, *e.g.*, outer energy calibration (the spectrometer is calibrated with calibration sources in one experiment and the spectrum with gamma line the energy of which is to be determined is measured in the next experiment). Nevertheless, the stability of line positions was checked during all our mesurements. If a larger change of the line positions or broadening of the lines was observed the measurement was rejected. Position instabilities of the line 9.4 keV, observed in channel 1320, determined from 6 ten-hour spectra measured within the period of 8 days were less than 0.6 channel. If the shift of the line 9.4 keV was detected then the adequate shifts were observed for the other lines, *i.e.* gain and DC level drift typical for the gamma spectroscopy chains had manifested. We expected sufficient linearity of the dependence energy-channel in the used narrow working region of channels 1150–1650. The linearity without irregularities in the range around channel 3000 was demonstrated in [31] where the same gamma spectrometer was used and the gamma-ray energy of 32151.7(5) eV was determined. The calibration measurement at two different gains were accomplished in order to check the linearity of the system.

2.1 Parasitic lines in the energy spectra

Possible additional gamma or X-ray lines of any origin in the region of interest, especially close to the calibration lines or to the measured 9.4 keV line, could distort the peaks and cause a systematic uncertainty in the value of $E_{9.4}$. We took measures in order to minimize such interferences.

First, the ^{83}Rb activity was radiochemically purified by chromatography. The purified activity was measured on a large HPGe detector. Only the γ-lines from the isotopes ^{83,84,86}Rb were present in the spectrum.

Second, "Rb-only" spectra with only the ^{83}Rb/^{83m}Kr source were measured separately on the Si(Li) detector with the statistics expected in the calibration spectra, see fig. 1. The aim was to check that the background in the energy region of the calibration 7.5 and 10.5 keV lines and the 9.4 keV line was free of other lines. The result was not quite satisfactory. In addition to the expected Kr Kα line and weak Kr Kα escape line[2] also weak KX-lines of Ni and a background line with energy 9.7 keV were present. The Ni X-rays originate from the gas target inner walls that are nickeled. The chromatography procedure was not efficient enough in removing the Ni from the ^{83}Rb water solution. These Ni X-rays do not interfere as the Ni Kα_1 line is used as the calibration line.

The origin of the 9.7 keV line was examined by introducing a 25 μm Ni foil between the ^{83}Rb/^{83m}Kr source and the detector. The intensity of the 9.4 keV line was reduced by a factor of $\sim$200 in correspondence with relevant attenuation coefficient, but the intensity of the 9.7 keV line was reduced only by a factor of $\sim$10, *i.e.* similarly as the strong Kr Kα radiation was attenuated. In further test, the spectrum of ^{81}Rb, void of 9.4 keV line and having also strong Kr Kα radiation, was measured. The

[2] The escape peak is a result of incomplete energy detection of the Kr Kα X-rays. A K electron of silicon is knocked out of the atom and the resulting fluorescence KX radiation of Si can leave the detector volume. In that case the original energy is reduced by energy of this fluorescence X-ray, which for silicon gives about 1.8 keV.

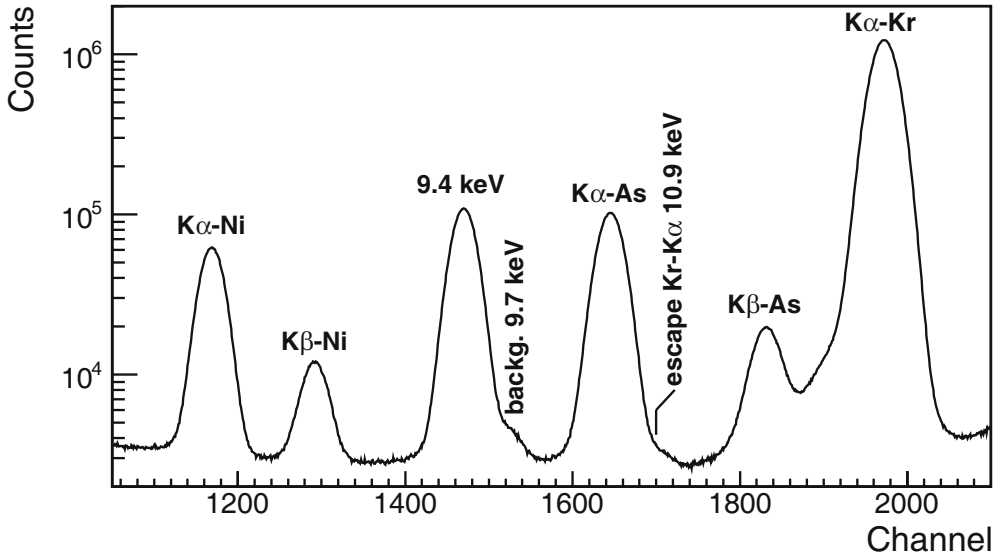

Fig. 2. Photon calibration spectrum in the vicinity of the 9.4 keV line measured with ^{83}Rb/^{83m}Kr and the fluorescent elements Ni and As.

9.7 keV line was again present in the spectrum, this time as a single line, with similar intensity (relative to Kr Kα) as in the spectrum with ^{83}Rb/^{83m}Kr source. It was concluded that the 9.7 keV line is induced by photons (predominantly by Kr Kα) from the radioactive source in the detector surrounding material. In separated measurement of the source on another detector (Silicon Drift Detector, company Amptek) the line 9.7 keV was not visible and the conclusion above about its origin was thus indirectly confirmed.

At a first glance this peak could be assigned to Au LX-rays arising by fluorescence on Au possibly present in detector surroundings, *i.e.* to a doublet of Lα_1 and Lα_2 with energies of 9713.44(34) and 9628.05(33) eV [24] and relative intensities 8.9 to 1 [34]. This parasitic line is weak. Any attempt to fit the 9.4 keV region with at least three Gaussian functions (9.4 line + doublet for the parasitic line) was unsuccessful —the doublet for the 9.7 keV lines converged to a single line. The fit of the region with one Gaussian and two Voigt functions (with fixed splitting and amplitude ratio taken from Au LX-rays tables) was also accomplished. The energy of the stronger component of 9.7 keV line was by 30 eV higher than the expected table value for the Lα_1. Nevertheless, the energy of the 9.4 keV line was close to that obtained when the fit with two Gaussian functions was applied within 0.05 eV. To study this problem further, in a special measurement the energy of the Au LX doublet induced in Au foil (purity 99.999%) by the photons from the ^{83}Rb/^{83m}Kr source situated aside of the alumina collimator (*i.e.* the photons from the source were not visible by the detector and the line 9.4 keV was missing in the spectrum) was determined. Obtained value of energy agreed with the energy for L$\alpha_{1,2}$ within 3 eV.

2.2 Shape of photon lines

The determination of the precise positions of the γ-ray and X-ray lines requires adequate description of the photon lines used in the spectrum fitting procedure. The line 9.4 keV originates in atomic nucleus while the calibration characteristic Kα_1 lines come from the atomic shell. A typical calibration spectrum is presented in fig. 2. Linear background was assumed under the peaks of interest. The instrumental line shape in the form of Gaussian function was used for the 9.4 keV γ-line. In case of X-ray lines Voigt functions were applied where the appropriate Lorentzian widths were calculated from the recommended widths of atomic levels [36]. For both types of photon lines also weak asymmetry component $S(E)$ (representing incomplete charge collection in the detector) according to [37] was used. This component is given by the expression $S(E) = 0.5\,A_S\,\exp[(E-E_{ph})/\beta]\,\mathrm{erfc}[(E-E_{ph})/(\sqrt{2}\sigma)+\sigma/(\sqrt{2}\beta)]$, where A_S is the amplitude relative to the amplitude of the main line, E_{ph} is the energy of the photon line, erfc is the complementary error function with parameters σ being the Gaussian function sigma parameter and β controlling the width of the component.

Besides, a more complicated structure of X-ray spectrum was taken into account. First, each Kα_1 line used for the calibration is accompanied by close lying Kα_2 line unresolved by the detector. In order to achieve reasonable and stable result of the fit the parameters of the Kα_2 line, position and amplitude relative to Kα_1, were deduced from the literature values of the energies and intensities [24,34] and held fixed in the fit. Explicit values for this ratio for Ni and As are 0.508(34) and 0.514(26), respectively [34]. In view of the proximity of both lines the influence of different detector efficiency on the am-

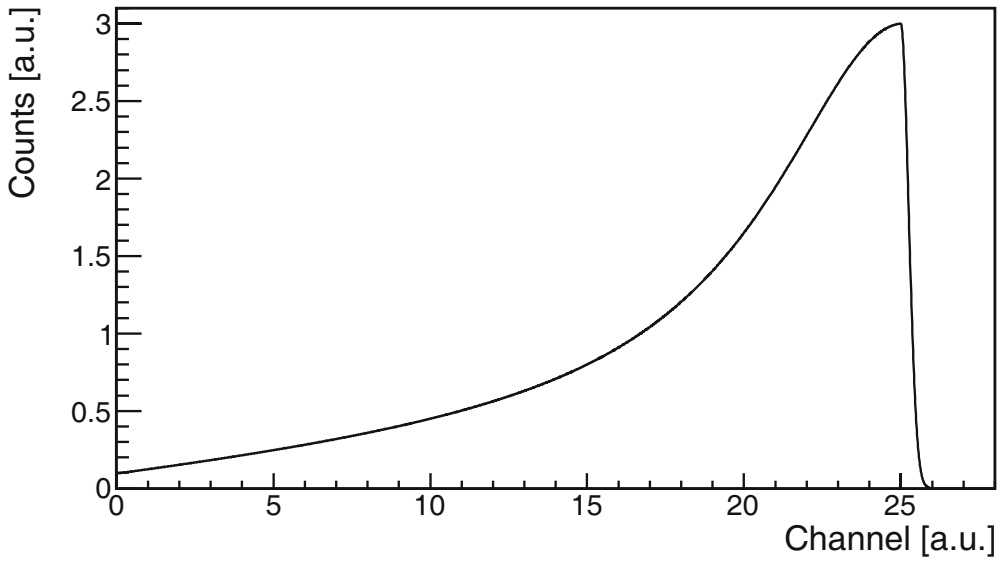

Fig. 3. The phenomenological shape of the RAE spectrum built up using the connection of the Lorentzian (soft low-energy side) and the Gaussian (steep high-energy side) functions.

plitude ratios was neglected. The fitted Gaussian σ was common for the both lines. Second, two tiny atomic shell features accompanied the main X-rays, namely the higher energy satellite lines (α_3, α_4 and α_3' with relative intensities to Kα_1 of about 0.002) and the spectra of the radiative Auger effect (RAE) (K-LM and K-MM with relative intensities to Kα_1 of about 0.005) were also considered. Both effects result in the emission of X-rays close to the Kα_1 and also unresolved by the detector. These X-rays were taken into account in the same way as the Kα_2 was with one exception. Due to the weak intensity of the both effects the asymmetry component $S(E)$ was omitted. The relevant data about the line energies, intensities and widths in case of satellite lines were taken from the works [38,39]. As for the energy and intensity uncertainties general values of 10^{-5} and less than 15%, respectively, can be found in the references. In the analysis (see sect. 2.3), the more conservative value of 25% was used for the intensity uncertainties. In the case of RAE, the intensities were found in the work [40]. As no theoretical description of the radiative Auger spectrum is available (the simple Gaussian shape was used in [41]) a phenomenological shape inspired by the experimental spectra of K-LM and K-MM in [42, 43] (the spectra of RAE were measured with high resolution on the bent crystal spectrometer) was constructed using the Lorentzian and Gaussian functions, see fig. 3. The boundaries of the shape were established as the energy interval spanned by K-LM or K-MM Auger electrons according to the semi-empirical values from [44]. Such a shape was convoluted with a Gaussian the σ of which was common to that used for the Voigt profile of the Kα_1. The RAE intensity and energy uncertainties are not indicated in the work [40]. In the analysis (see sect. 2.3) was used for the intensity the value of 25% based on the intensities scatter in [40]. The uncertainty of the Auger electron energies from [44] amounting to 2 eV was accepted as an uncertainty of the RAE shape boundaries.

The background 9.7 keV and escape Kr Kα lines creating doublets with the 9.4 keV and As Kα lines, respectively, were described by a single Gaussian where its parameters for position, amplitude and σ were fitted independently on the 9.4 keV and As Kα lines.

2.3 Calibration and fitting procedure, systematic uncertainty of $E_{9.4}$

In the calibration spectra three regions were fitted separately: the Ni calibration line (plus Kα_2, RAE spectrum, satellite lines), the calibrated line 9.4 keV (plus background line 9.7 keV) and the As calibration line (plus Kα_2, RAE K-LM spectrum, satellite lines, escape Kr Kα). The fits were done in the framework ROOT [45] using the Minuit library. The linear dependence of energy on the channel number was used for the calculation of the $E_{9.4}$ value.

For the fit of the Kα regions the energy difference between Kα_1 and other X-rays (Kα_2, satellites, RAE lines) and the values of Lorentzian widths had to be converted into units of channels. For this, the fitting procedure was constructed as follows. First, the Ni and As Kα doublet positions were determined in the fit using the single Gaussians and the corresponding difference in the positions $\Delta_p[channel]$ was calculated. Then the intensity weighted mean values of table energies Kα_1 and Kα_2 for Ni and As were calculated and relevant $\Delta_E[eV]$ was established. The starting value of the conversion factor was obtained as Δ_p/Δ_E. Second, using the starting conversion factor

Table 1. Individual and total systematic uncertainties of $E_{9.4}$.

Parameter	Contribution [eV]
Energy difference of Kα_1 and Kα_2	0.030
Amplitude ratio of Kα_1 and Kα_2	0.275
Energy difference of Kα_1 and satellite lines	0.001
Amplitude ratio of Kα_1 and satellite lines	0.015
Energy difference of RAE peak and Kα_1	0.002
Amplitude ratio of RAE peak and Kα_1	0.063
Total	0.28

the full fit of Ni and As regions (Kα_2 and remaining components) was done. The obtained positions of Ni and As Kα_1 were used for the determination of improved value for the conversion factor, this time using Ni and As Kα_1 table energies. The second step was repeated until convergence of fitted parameters, the conversion factor including, was achieved.

The asymmetry component parameters A_S and β were held fixed in fits of the calibration spectra and were obtained in the following way. The "fluorescent" spectra of both Ni and As calibration lines were acquired separately by placing the ^{83}Rb/^{83m}Kr source aside so that no radiation from it could reach the detector. As such spectra were clear of any other lines the asymmetry component parameters could be obtained more reliably by the fit from them. Similarly, the parameters A_S and β for the 9.4 keV line were obtained from the simpler Rb-only spectra. Values for A_S relatively to amplitude of the corresponding line range typically from 0.02 to 0.05 and values for β range typically from 16 to 30 in units of channels.

Beside a standard fitting of the calibration spectrum in Ni and As regions an alternative approach was used for taking into account a small non-linear background in the region of Ni KX-rays and the weak Kr Kα escape line (having actually a complicated structure, see [46]) on the positions of the calibration lines. An Rb-only spectrum was measured under the same conditions as a calibration spectrum. Then a spectrum, called "subtracted", was created in a way that in each channel the number of counts was taken as difference between the counts in the calibration and Rb-only spectra. Finally, the subtracted spectrum, practically free of escape line and non-linear background, was fitted. As for the Ni region, the amount of Ni impurity in the source was small enough, so that only a small fraction of the original line amplitude is subtracted.

The systematic uncertainty of $E_{9.4}$ was determined from systematic uncertainties of the fitted positions for the Ni and As Kα_1 calibration lines. The systematic uncertainty of the Kα_1 position was taken as the width of the Gaussian distribution of the positions which were obtained from a total of 10^4 fits. For each fit, the necessary parameters of the calibration line were taken randomly according to the Gaussian distributions, the width of which were equal to the standard deviations of the parameters.

Table 2. The $E_{9.4}$ value from the four measurements.

No.	Gain	$E_{9.4}$[eV]
1	Smaller	9405.85(9)
2		9405.78(9)
3	Larger	9405.77(10)
4		9405.89(11)
	Mean	9405.82(5)

The varied parameters were: energy difference and amplitude ratio of Kα_2 and Kα_1, energy difference and amplitude ratio of satellite lines and Kα_1, energy difference and amplitude ratio of RAE peak and Kα_1. As a result, the systematic uncertainty of 0.28_{syst} eV was obtained. The parameter, the uncertainty of which contributed to the systematic uncertainty by the largest amount, was found to be the amplitude ratio of the Kα_2 and Kα_1. For individual contributions to the systematic uncertainty of $E_{9.4}$ see table 1.

3 Result of calibration measurements

The values of $E_{9.4}$ obtained from the four measurements are presented in table 2. In order to verify the linear dependence of the energy on the channel number the value $E_{9.4}$ was obtained in two phases which differed in the amplifier gain. The difference amounted to 5% giving a shift of 100 channels in the region of interest. In each phase, two calibration spectra were acquired. An Rb-only spectrum for the analysis by the subtracted spectrum method was always measured right after the calibration spectrum, in order to minimize any possible change of the amplifier gain. Good agreement between the results of both gains is obvious.

The Ni Kα and As Kα line regions were fitted via both standard and subtraction methods. In the case of the Ni Kα line region and subtraction method additionally Kβ lines and respective K-MM RAE spectrum were fitted. In order to keep the fit stable, these additional contributions were included in the fit using their positions and

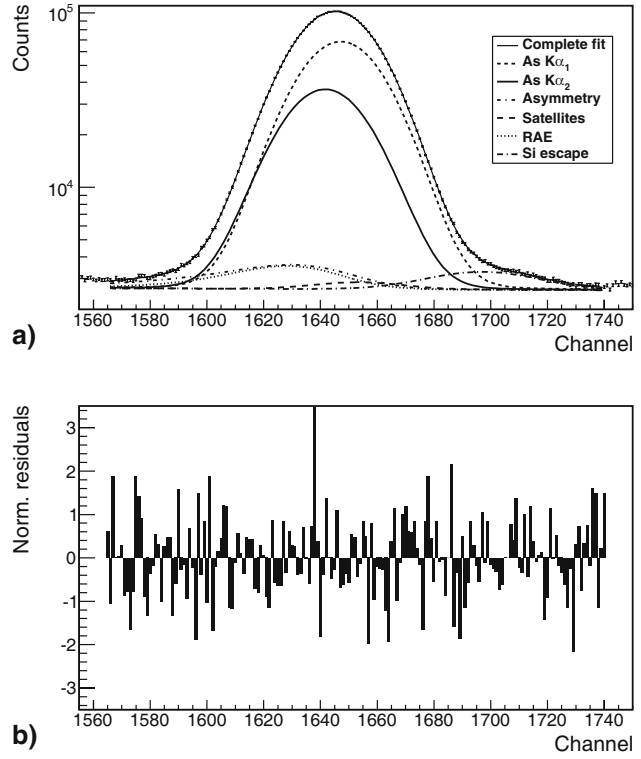

Fig. 4. Result of the standard analysis of the As Kα region with the experimental spectrum and its individual components (a). The normalized residuals are also shown (b). In this fit $\chi^2_{\rm dof} = 0.9$ (168 dof).

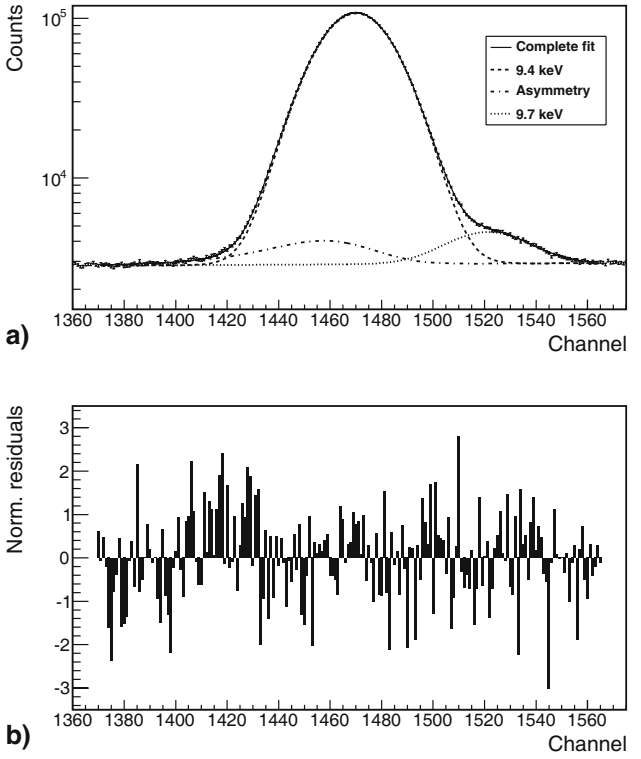

Fig. 5. Result of the analysis for the 9.4 keV line region with the experimental spectrum and its individual components (a). The normalized residuals are also shown (b). In this fit $\chi^2_{\rm dof} = 1.0$ (188 dof).

amplitudes relative to Ni Kα_1 as was explained in subsect. 2.2 for the Kα_2 and K-LM cases. The application of the subtraction method resulted in the residual plot without structures —the value of $\chi^2_{\rm dof}$ was reduced typically from $\chi^2_{\rm dof} = 1.4$ (298 dof) (standard method) to $\chi^2_{\rm dof} = 1.1$ (298 dof). In the case of the As Kα line region, both methods gave very similar values of $\chi^2_{\rm dof}$ of about typically 1.1(168 dof) —the residual plots were without the structures. An example of the As Kα line region analysis is shown in fig. 4. The region of the 9.4 keV line was fitted by the standard method with typical value of $\chi^2_{\rm dof} = 1.2$ (188 dof). An example of the result including residuals is shown in fig. 5. In spite of the two different approaches to the Ni and As regions, both methods resulted in values of $E_{9.4}$, which differed by only 0.08 eV. For this reason only the values obtained from the standard approach are presented in table 2.

4 Discussion

The influence of the RAE effect on the $E_{9.4}$ value was important. The omission of it caused increase of the 9.4 keV transition energy by 0.3 eV. On the other side, when the X-ray satellite lines were not taken into account, the measured energy was reduced, but only by 0.1 eV. Our result for $E_{9.4}$ value $9405.82 \pm 0.05_{\rm stat} \pm 0.28_{\rm sys}$ eV is in agreement with the previous less precise γ-spectrometry results and the precise electron spectroscopy measurement of the work [8] (9405.9 ± 0.8 eV). When compared with the electron spectroscopy value published in [29] 9404.71 ± 0.35 eV our value is the same in the frame of two standard deviations.

5 Conclusion

In this work the precise energy of the 9.4 keV γ-transition in the ^{83}Rb decay was measured and found to be $E_{9.4} = 9405.8 \pm 0.3$ eV. The energy value was obtained using the Si(Li) photon spectrometry measurements of differences in the energy with respect to the closely spaced characteristic X-ray lines. This result allows the determination of the precise energies of the 9.4 keV conversion electrons intended for the systematic measurement at the neutrino mass experiment KATRIN.

This work was supported by the MŠMT grants LC07050, SVV-2011-263309, MSM6840770040, GAČR grant P203/12/1896 and by the Academy of Sciences of the Czech Republic under contract IRP AV0Z10480505.

References

1. K. Nakamura, K. Hagiwara *et al.*(Particle Data Group), J. Phys. G **37**, 075021 (2010) http://pdg.lbl.gov, doi:10.1088/0954-3899/37/7A075021.
2. Ch. Kraus, B. Bornschein, L. Bornschein, J. Bonn, B. Flatt, A. Kovalik, B. Ostrick, E.W. Otten, J.P. Schall, Th. Thümmler, Ch. Weinheimer, Eur. Phys. J. C **40**, 447 (2005) doi:10.1140/epjc/s2005-02139-7.
3. V.N. Aseev, A.I. Belesev, A.I. Berlev, E.V. Geraskin, A.A. Golubev, N.A. Likhovid, V.M. Lobashev, A.A. Nozik, V.S. Pantuev, V.I. Parfenov, A.K. Skasyrskaya, F.V. Tkachov, S.V. Zadorozhny, Phys. Rev. D **84**, 112003 (2011) doi:10.1103/PhysRevD.84.112003.
4. J. Angrik, T. Armbrust *et al.*, KATRIN Design Report 2004, Report NPI ASCR Řež EXP-01/2005 or FZKA Scientific Report 7090, Karlsruhe, http://www-ik.fzk.de/tritium/publications/index.html.
5. R.G.H. Robertson, T.J. Bowles, G.J. Stephenson jr., D.L. Wark, J.F. Wilkerson, Phys. Rev. Lett. **67**, 957 (1991) doi:10.1103/PhysRevLett.67.957.
6. W. Stoeffl, D.J. Decman, Phys. Rev. Lett. **75**, 3237 (1995) doi:10.1103/PhysRevLett.75.3237.
7. A. Picard, H. Backe, H. Barth, J. Bonn, B. Degen, Th. Edling, R. Haid, A. Hermanni, P. Leiderer, Th. Loeken, A. Molz, R.B. Moore, A. Osipowicz, E.W. Otten, M. Przyrembel, M. Schrader, M. Steininger, Ch. Weinheimer, Nucl. Instrum. Methods Phys. Res. B **63**, 345 (1992) doi:10.1016/0168-583X(92)95119-C.
8. A. Picard, H. Backe, J. Bonn, B. Degen, R. Haid, A. Hermanni, P. Leiderer, A. Osipowicz, E.W. Otten, M. Przyrembel, M. Schrader, M. Steininger, Ch. Weinheimer, Z. Phys. A Hadr. Nucl. **342**, 74 (1992) doi:10.1007/BF01294491.
9. V.N. Aseev, A.I. Belesev, A.I.Berlev, E.V. Geraskin, O.V. Kazachenko, Yu.E. Kuznetsov, V.M. Lobashev, R.P. Ostroumov, N.A. Titov, S.V. Zadorozhny, J. Bonn, B. Bornschein, L. Bornschein, E.W. Otten, M. Przyrembel, Ch. Weinheimer, A. Saenz, Eur. Phys. J. B **10**, 39 (2000) doi:10.1007/s100530050525.
10. B. Bornschein, J. Bonn, L. Bornschein, E.W. Otten, Ch. Weinheimer, J. Low Temp. Phys. **131**, 69 (2003) doi:10.1023/A:1022805313162.
11. S. Väisälä, G. Graeffe, J. Heinonen, A.A. Delucchi, R.A. Meyer, Phys. Rev. C **13**, 372 (1976) doi:10.1103/PhysRevC.13.372.
12. F. Rösel, H.M. Fries, K. Alder, H.C. Pauli, At. Data Nucl. Data Tables **21**, 91 (1978) doi:10.1016/0092-640X(78).
13. V. Pantuev, NRI Troick, private communication (2011).
14. C.E. Moore, *Atomic Energy Levels*, in National Stand. Ref. Data Ser., Vol. **III** (National Bureau of Standards, 1958) Cir. 467.
15. K. Codling, R.P. Madden, Phys. Rev. Lett. **12**, 106 (1964) doi:10.1103/PhysRevLett.12.106.
16. W. Mehlhorn, Z. Phys. **187**, 21 (1965) doi:10.1007/BF01380902.
17. R. Spohr, T. Bergmark, N. Magnusson, K. Siegbahn, University of Uppsala, Prelim. Rep. Oct. 1967.
18. K. Siegbahn, C. Nordling, G. Johansson, J. Hedman, P.F. Hedén, K. Hamrin, U. Gelius, T. Bergmark, L.O. Werme, R. Manne, Y. Baer, *ESCA applied to free molecules* (North Holland, Amsterdam, 1969).
19. W.S. Watson, F.J. Morgan, J. Phys. B: Atom. Molec. Phys. **2**, 277 (1969) doi:10.1088/0022-3700/2/2/316.
20. G. Johansson, J. Hedman, A. Berndtsson, M. Klasson, R. Nilsson, J. Electr. Spec. Rel. Phen. **2**, 295 (1973) doi:10.1018/0368-2048(73)80022-2.
21. G.C. King, M. Tronc, F.H. Read, R.C. Bradford, J. Phys. B: Atom. Molec. Phys. **10**, 2479 (1977) doi:10.1088/0022-3700/10/12/026.
22. J.A. Bearden, A.F. Burr, Rev. Mod. Phys. **39**, 125 (1967) doi:10.1103/RevModPhys.39.125.
23. K.D. Sevier, Atom. Data Nucl. Data Tables **24**, 323 (1979) doi:10.1016/0092-640X(79)90012-3.
24. R.D. Deslattes, E.G. Kessler jr., P. Indelicato, L. de Billy, E. Lindroth, J. Anton, Rev. Mod. Phys. **75**, 35 (2003) doi:10.1103/RevModPhys.75.35.
25. O. Dragoun, A. Špalek, F.J. Wuilleumier, Czech J. Phys. **54**, 833 (2004) doi:10.1023/B:CJOP.0000038591.13369.e1.
26. S.L. Ruby, R.G. Klark, L.E. Glendenin, Phys. Lett. A **36**, 321 (1971) doi:10.1016/0375-9601(71)90529-9.
27. B. Kolk, F. Pleiter, W. Heeringa, Nucl. Phys. A **194**, 614 (1972) doi:10.1016/0375-9474(72)91007-X.
28. A. Kovalik, V.M. Gorozhankin, J. Phys. G: Nucl. Part. Phys. **19**, 1921 (1993) doi:10.1088/0954-3899/19/11/018.
29. B. Ostrick, PhD Thesis, Münster University (2008) http://www-ik.fzk.de/tritium/publications/thesis.html.
30. T. Mandel, M. Domke, G. Kaindl, C. Laubschat, M. Priestch, U. Middelmann, K. Horn, Surf. Sci. **162**, 453 (1985) doi:10.1016/0039-6028(85)90935-5.
31. D. Vénos, O. Dragoun, A. Špalek, M. Vobecký, Nucl. Instrum. Methods A **560**, 352 (2006) doi:10.1016/j.nima.2005.12.213.
32. K. Debertin, R.G. Helmer, *Gamma- and X-ray spectrometry with semiconductor detectors* (North-Holland, 1988) p. 194.
33. Y.A. Akovali, Nucl. Data Sheets **74**, 461 (1995) doi:10.1006/ndsh.1995.1014.
34. R.B. Firestone, V.S. Shirley, C.M. Baglin, S.Y. Frank Chu, J. Zipkin, *Table of Isotopes*, Eighth edition (Wiley, New York, 1996, 1998 (update)).
35. D. Vénos, A. Špalek, O. Lebeda, M. Fišer, Appl. Radiat. Isot. **63**, 323 (2005) doi:10.1016/j.apradiso.2005.04.011.
36. J.L. Campbell, T. Papp, At. Data Nucl. Data Tables **77**, 1 (2001) doi:10.1006/adnd.2000.0848.
37. J.L. Campbell, B.M. Millman, J.A. Maxwell, A. Perujo, W.J. Teesdale, Nucl. Instrum. Methods B **9**, 71 (1985) doi:10.1016/0168-583X(85)90780-3.
38. L.G. Parratt, Phys. Rev. **50**, 1 (1936) doi:10.1103/PhysRev.50.1.
39. C.H. Shaw, L.G. Parratt, Phys. Rev. **50**, 1006 (1936) doi:10.1103/PhysRev.50.1006.
40. A. Mühleinsen, M. Budnar, J.Cl. Dousse, Phys. Rev. A **54**, 3852 (1996) doi:10.1103/PhysRevA.54.3852.
41. J.L. Campbell, A. Perujo, W.J. Teesdale, B.M. Millman, Phys. Rev. A **33**, 2410 (1986) doi:10.1103/PhysRevA.33.2410.

42. Ch. Herren, J.Cl. Dousse, Phys. Rev. A **53**, 717 (1996) doi:10.1103/PhysRevA.53.717.
43. Ch. Herren, J.Cl. Dousse, Phys. Rev. A **56**, 2750 (1997) doi:10.1103/PhysRevA.56.2750.
44. F.P. Larkins, At. Data Nucl. Data Tables **20**, 311 (1977) doi:10.1016/0092-640X(77)90024-9.
45. ROOT, *Object-Oriented Data Analysis Framework*, `http://root.cern.ch` (2011).
46. J.L. Campbell, J.A. Maxwell, T. Papp, G. White, X-ray Spectrom. **26**, 223 (1997) doi:10.1002/ (SICI)1097-4539(199707)26:4<223::AID-XRS224>3.0.CO;2-8.